Geodynamic Evolution of Sedimentary Basins, International Symposium.
© F. Roure, N. Ellouz, V.S. Shein, I. Skvortsov ed. and Editions Technip.
Moscow, 1994, pp. 203-218
27 rue Ginoux, 75015 Paris

THE BOOMERANG-CHAPARE TRANSFER ZONE (Recent Oil Discovery Trend in Bolivia): STRUCTURAL INTERPRETATION AND EXPERIMENTAL APPROACH

P. Baby[1], M. Specht[2], J. Oller[3], G. Montemurro[3],
B. Colletta[2], J. Letouzey[2]

ABSTRACT

The central part of the Bolivian Andean fold and thrust belt is characterized by the existence of lateral and oblique ramps offsetting its front. The Boomerang-Chapare transfer zone, north of Santa Cruz, is the most dramatic in so far as it provokes a hundred-kilometer sinistral offset of the Andean thrust front.

Combined surface and subsurface data have been used here to present an up-to-date structural and kinematic model of the Boomerang-Chapare transfer zone. Moreover, a set of analog modeling in a sandbox has enabled us to test our hypotheses and study the propagation of the thrusts. The 3D visualization of the deformed model was done by computerized X-ray tomography.

We thus show that the main decollement level is located at the bottom of a Paleozoic sedimentary wedge lying on the Brazilian shield and that geometry of the border of the detached wedge is what governs and situates the development of the transfer zone. The relation between thrust propagation sequence and location of oil fields is then examined.

INTRODUCTION

In they central part, the Andes form a bend (Fig. 1a) called the Bolivian Orocline (Carey, 1958; Isacks, 1988). This bend occurs between 16°S and 18°S (Fig. 1b) and is characterized by large transfer zones.

Transfer zones have been defined by Dahlstrom (1969) as zones where a displacement is transferred from one structure to another. This mechanisms, which induces noncylindrical structures, has been described in most of the frontal part of thrust belts, but its causes have seldom been studied owing to the lack of constraints for the deep structure of the zones.

South of Santa Cruz (between 17.5°S and 18°S), the front of the N-S orientated Subandean zone shows classic thrusting structures (Figs 1b, 2a and 2b). More to the north (between 16°S and 17,5°S), it changes to a NW-SE direction and becomes more complex (Figs. 2c and 2d). In this zone, the geometry and the shortening percentage of the foreland thrust system show large lateral variations. These lateral variations in shortening, which are illustrated by the balanced cross-sections

(1) ORSTOM, CC 4875, Santa Cruz, Bolivia..
(2) Institut Français du Pétrole, BP 311, 92506 Rueil-Malmaison Cedex, France.
(3) YPFB - GXG, CC 1659, Santa Cruz, Bolivia.

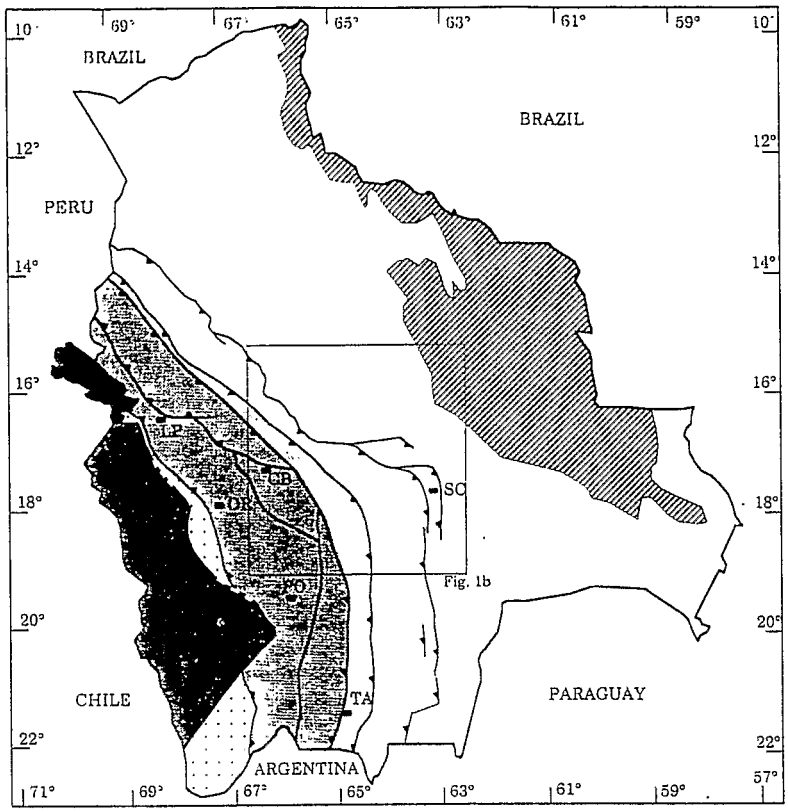

FIG. 1a. Tectonic map of Bolivia (Bolivian Orocline) and location of the Boomerang-Chapare area.

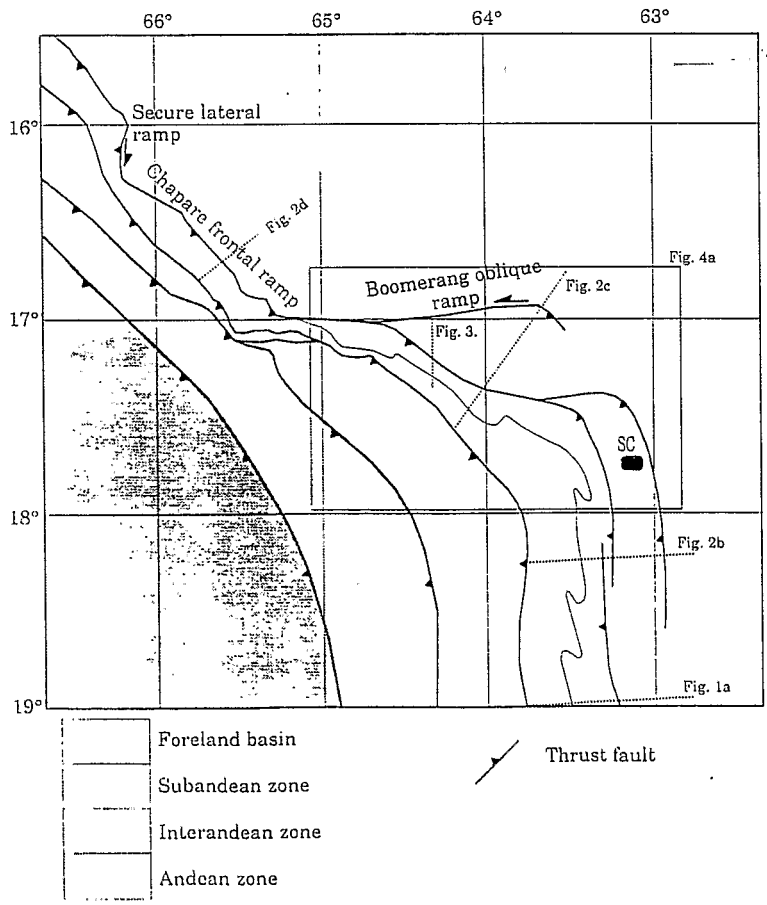

FIG. 1b. Structural map of the Boomerang-Chapare area.

in Fig. 2, are accommodated by the transfer zone of the Boomerang-Chapare area.

The Boomerang-Chapare region corresponds to the latest oil discovery play found in Bolivia. It examplifies a transfer zone whose deep structure is well constrained by subsurface data. In this paper, we propose to describe the structural geometry of the Boomerang-Chapare area along with the kinematic model of the deformation deduced from the geological study as well as analog sandbox experiments carried out to test our model. The analog sandbox experiments were performed and analyzed by computerized X-ray tomography at the Institut Français du Pétrole. Well and seismic reflection data were provided by the Bolivian State Oil Company (Yacimientos Petroliferos Fiscales Bolivianos).

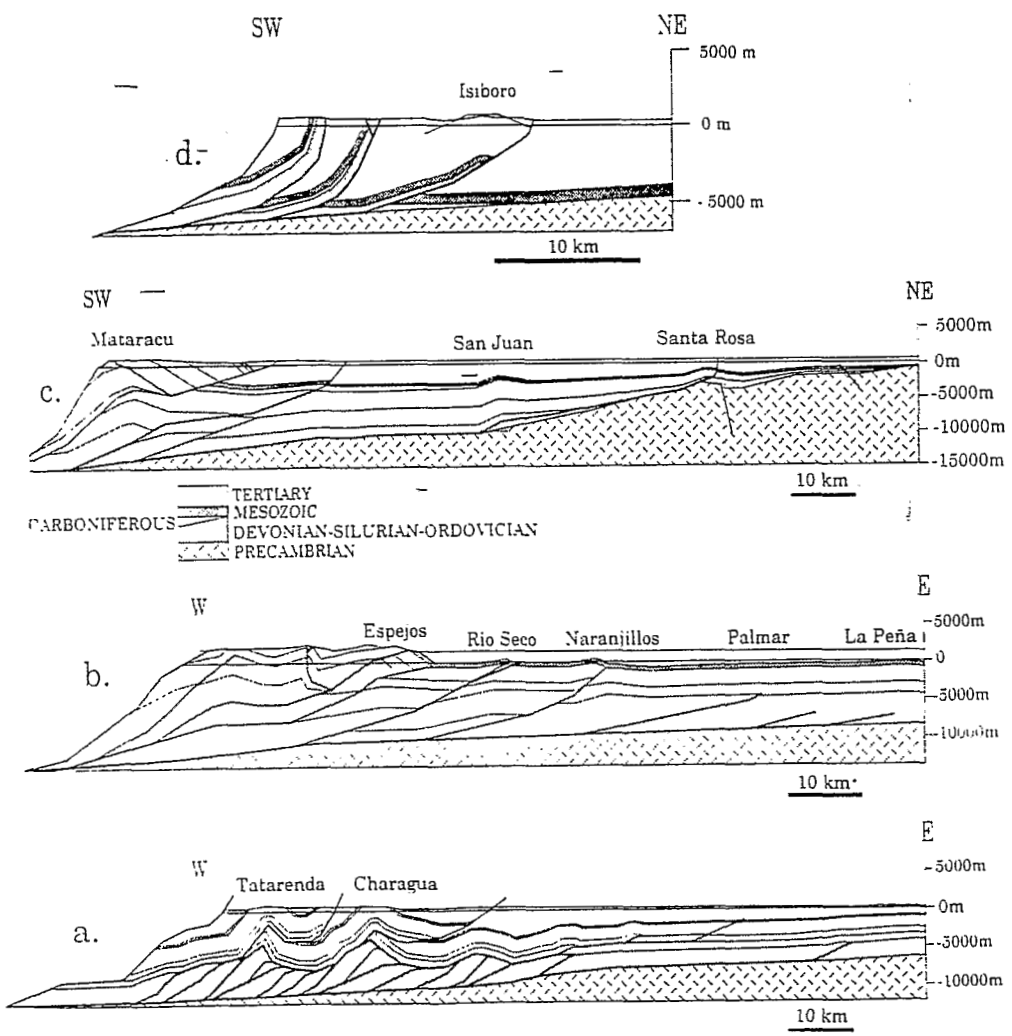

FIG. 2. Three regional balanced cross-sections in the eastern part of the Subandean Zone (location in Fig. 1b):

(a) In the Southern Subandean Zone (19°S).
(b) South of the Boomerang area (18°S).
(c) In the Boomerang area.
(d) In the Chapare area.

1. GEOLOGIC AND GEOPHYSICAL SETTING OF THE BOOMERANG-CHAPARE AREA

1.1 Stratigraphy and Major Decollement Level

The sedimentary pile involved in thrusting in the Boomerang-Chapare area is characterized by large lateral variations in thickness. The synthetic stratigraphic log (Fig. 3) reveals the following tectono-stratigraphic units: a thick (up to more than 5,000 meters) Paleozoic sedimentary wedge consisting of a continuous series ranging from Ordovician to Carboniferous and thinning northwards lies on the Precambrian Brazilian shield, made of more competent rocks. This sedimentary wedge is itself unconformably covered by an isopachous series of 500 meters of Mesozoic and more than 1,600 meters of Oligocene to Pleistocene foreland deposits (Padulà, 1959; Lopez, 1974). The northward thinning of the Paleozoic prism is due to both the onlapping of the series on the Brazilian shield and the truncation of the top of this sedimentary wedge under the Mesozoic angular unconformity. North of the Boomerang thrust, there is no trace of the Paleozoic, and the Mesozoic sediments lies directly on the top of the Precambrian substratum. The major decollement level is located in the basis of the Paleozoic sedimentary wedge.

1.2 Structure of the Boomerang-Chapare Area

In the frontal part of the Bolivian Andean fold and thrust belt, the deformation began in Upper Oligocene times and is still in progress (Martinez, 1981; Oller, 1986; Isacks, 1988; Sheffels. 1988; Baby et al., 1989, 1992; Sempere et al., 1990). The Boomerang structures represent only one part of the entire Subandean plain strain of Neogene age. They hardly outcrop but

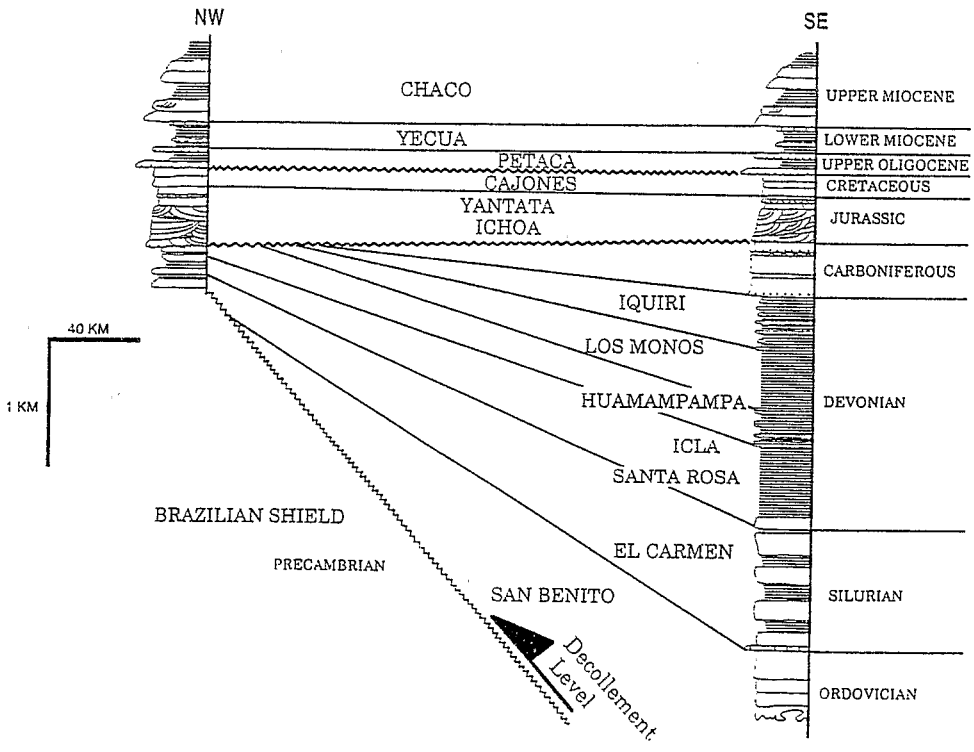

FIG. 3. Lithostratigraphy of the Paleozoic sedimentary wedge of the Boomerang-Chapare area (location in Fig. 1b).

are made conspicuous by seismic reflection surveying and are well constrained by oil well data. Among the thousands of kilometers of unmigrated and migrated seismic reflection profiles which cover the Boomerang area, the best profiles have been selected to construct structural sections across the major drilled structures and to draw isobath and isopachous structural maps. Figure 4a shows an isobath map of the top of the Mesozoic. Since the deformation of the Andean front started during Upper Oligocene, this map corresponds to the structural map of the Andean deformation. It makes clear that, at the top of the Mesozoic, most of the thrusts are blind and that the anticlines are generally fault-propagation folds. The SW-NE direction of the Andean compression revealed by this map is reminiscent of that of the structures and microstructures observed in the outcropping part of the fold and thrust belt south of Boomerang. The E-W orientated northern border of the Boomerang area corresponds to a complex deformation front standing with an oblique angle to the direction of the regional shortening. This deformation front, which is therefore an oblique ramp, abruptly dies away eastward in a very short E-W frontal structure (Palometas anticline). Farther south, the deformation front is found 35 km backward, and the structures become frontal again in relation to the regional shortening direction (Caranda anticline). Using seismic profiles, we were able to construct regional sections across the major drilled structures. These cross-sections show that, due to the strike-slip component along the Boomerang oblique ramp, the NE-SW oblique structures located all along this ramp are narrow and associated with high-angle faults (Figs 4b and 4c), whereas the NW-SE frontal structures are wide and spaced out and develop on low-angle thrust faults (Fig. 4d).

On a regional scale (Fig. 1b), the complex Boomerang thrust front then corresponds to an E-W oblique

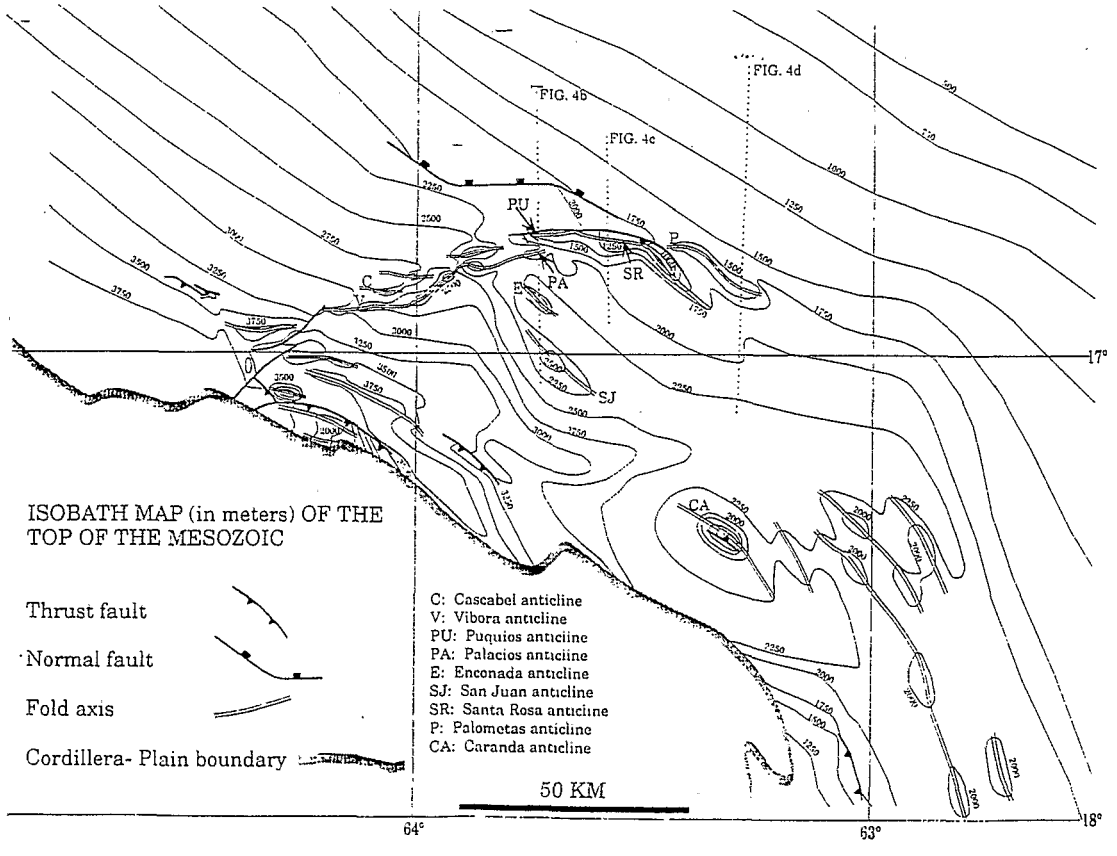

FIG. 4a. Isobath structural map of the top of the Mesozoic in the Boomerang area.

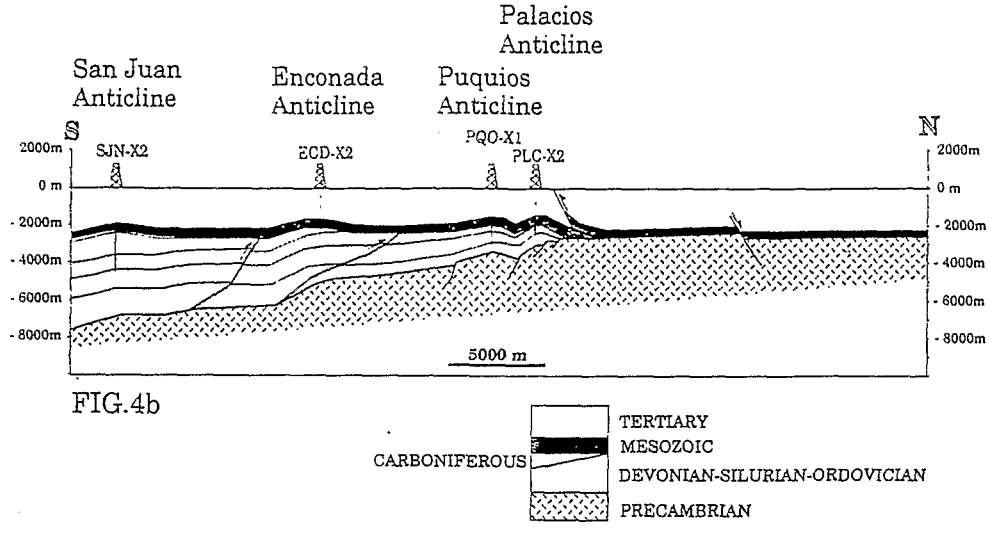

FIG.4b

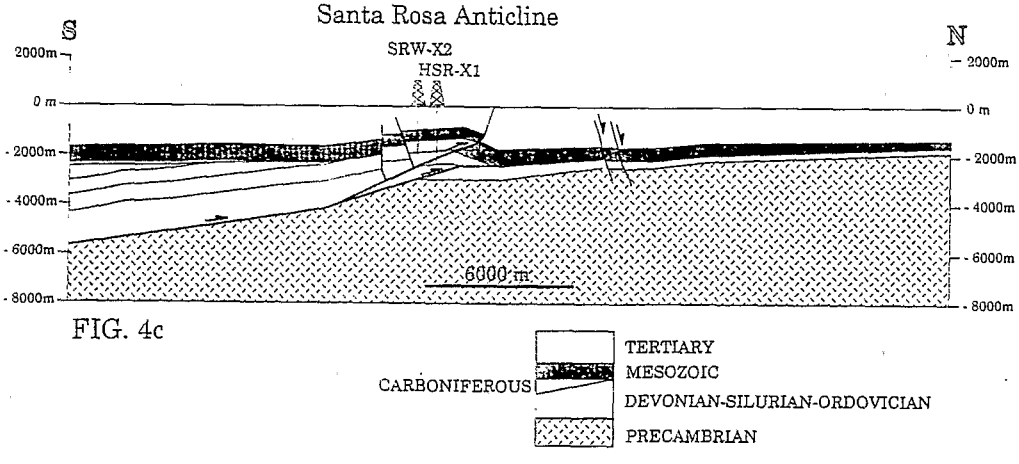

FIG. 4c

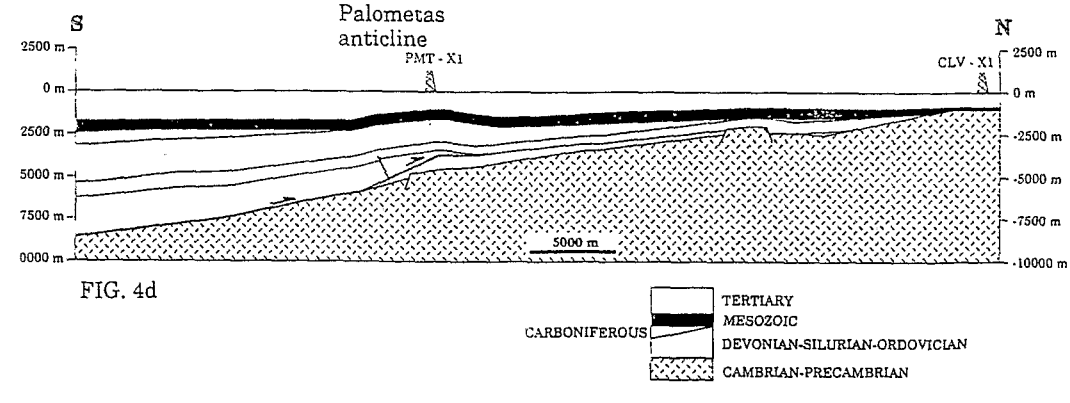

FIG. 4d

FIG. 4b, c, d. Structural sections across the frontal structures of Enconada and San Juan and across the Boomerang oblique ramp (Palacios and Puquios anticlines, Santa Rosa anticline, Palometas anticline).

ramp which, in the west, connects with the Chapare frontal ramp and, in the east, abruptly ends in a short frontal ramp.

1.3 Origins of the Boomerang-Chapare Trend and Constraints as to its Deep Structure

The structural cross-sections in Figs 2 and 4 show that the structures of the Boomerang area are included in an imbricate thrust system whose basal decollement is located at the bottom of the Paleozoic sedimentary wedge. A cause and effect relationship is therefore most likely to exist between the 3D geometry of the Paleozoic wedge (depth of the decollement level) and the geometry of the Andean thrust structures. In order to study this relation, we have drawn the isopachous map of the Paleozoic basin using seismic and well data (Fig. 5a). The relation between the deformation and the Paleozoic wedge geometry becomes clear when this map is superimposed on the structural map (Fig. 5b). We can see that the Boomerang oblique ramp coincides with the border of the Paleozoic wedge. The Boomerang-Chapare transfer zone can therefore be interpreted as an oblique ramp whose propagation was guided by the northern border of a Paleozoic sedimentary wedge, obliquely orientated *vis-à-vis* the regional shortening direction. On its eastern edge, the Boomerang oblique ramp ends in a short frontal structure developing towards the deeper part of the Paleozoic basin. Two hundred kilometers east of the Boomerang, this border outcrops (Paleja & Ballon, 1978) and stretches on in a WNW-ESE direction as far as Brazil. West of the Boomerang, it disappears under the Chapare frontal thrust.

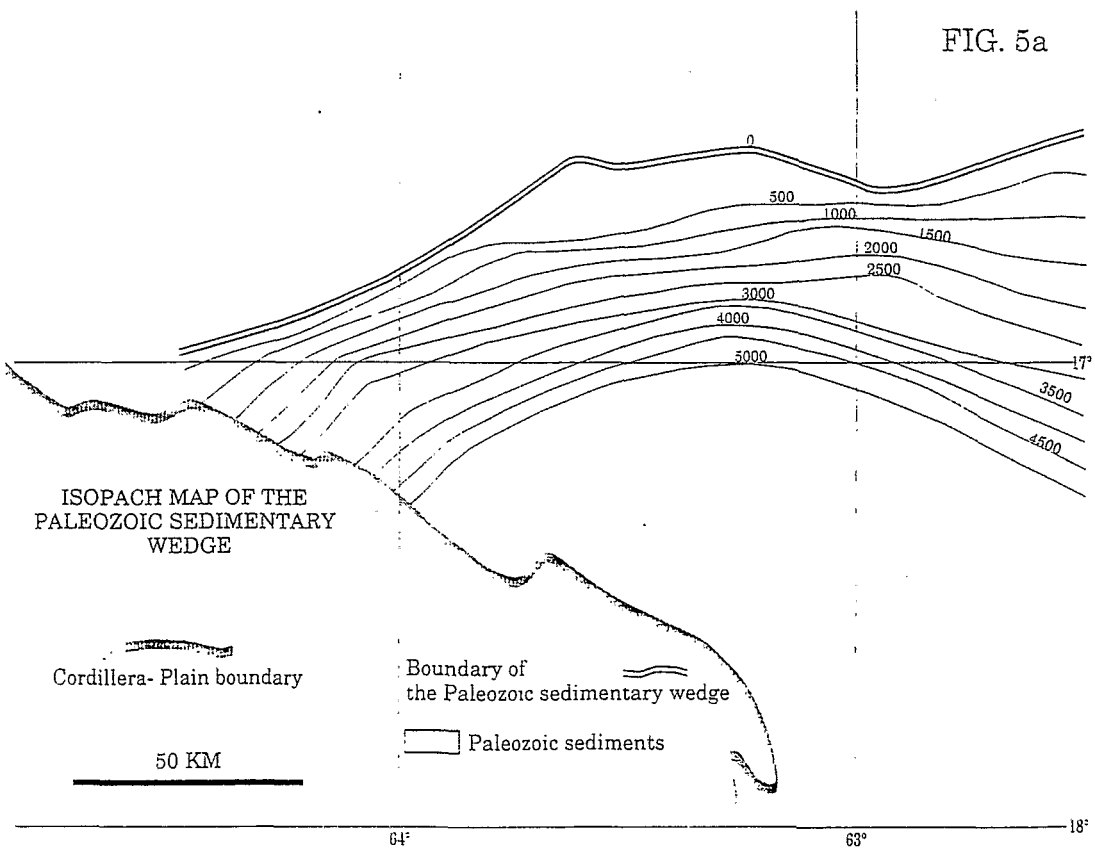

FIG. 5a. Isopachous map of the Paleozoic sedimentary wedge of the Boomerang area.

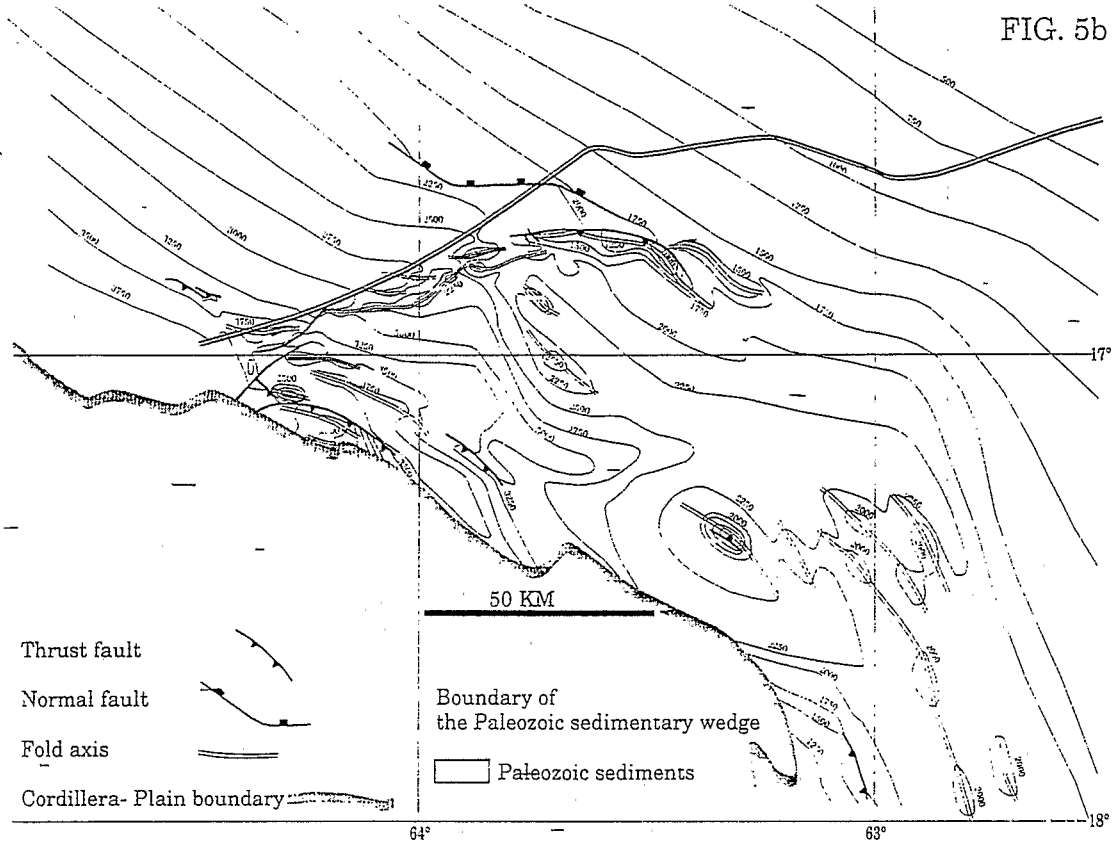

FIG. 5b. Structural map of the Boomerang area is superimposed on the isopachous map of the Paleozoic sedimentary wedge.

2. EXPERIMENTAL APPROACH

To test the interpretation of the Boomerang-Chapare transfer zone's origin, to constrain the boundary conditions and to study the thrust propagation sequence, we performed a set of analogic modeling whose 3D visualization was obtained thanks to computerized X-ray tomography. These experiments consisted in the making of normal gravity models (Malavielle, 1984), which were gradually shortened in a deformation box called Structurator, designed and built at the Institut Français du Pétrole. The principles and the technical details of this type of modeling and of its 3D analysis by computerized X-ray tomography are described in Colletta et al., 1991.

2.1 Model Setup

The rigid bottom of the deformation box was designed so as to reproduce the lateral variations of the decollement depth at the bottom of the Paleozoic series (Fig. 5a). Accordingly, we added a wooden plate simulating the rigid Precambrian substratum of the Paleozoic wedge. This wooden plate placed in the center of the box enabled us to simulate three types of wedge borders:

(a) The first one reproduces the border that had been established by the seismic mapping of the Boomerang area. It stands at a 40° angle to the shortening direction and has a dip of 10°.

(b) The second one has the same cross-section geometry as the first one but is orientated perpendicular to the shortening direction. It represents the substratum of the Paleozoic basin as it should be beneath the imbrication of the frontal thrusts of the Chapare area (Fig. 2d).
(c) The third one, cross cutting the previous one, is vertical and parallel to the shortening direction. It was intended to model the Secure transfer zone (Fig. 1b).

In the various modelings we performed, the basal decollement was enhanced either by microbeads (characterized by a low internal friction angle of about 20°) or silicone putty, except for the top of the wooden plate where sandpaper was used to simulate the lack of a decollement level north of the Boomerang oblique ramp. The Paleozoic sedimentary wedge and the Mesozoic and Cenozoic strata were modeled by several superimposed layers of sand and glass-powder. These two materials, whose deformation is described by the Mohr-Coulomb failure criteria, have very similar mechanical characteristics (cohesionless; internal friction angle of 33°). However, they have different X-ray attenuations, which makes it possible to image, under a scanner, the distinct layers of the sand and glass-powder layer-cake. The whole model is shown in Fig. 6. This model was then shortened by moving one of the walls (mobile backstop).

2.2 Results

Several experiments were performed: three with silicone putty and one with microbeads. The three modeling sequences with silicone putty were performed with different shortening velocities (1, 2 and 4 cm per hour). In all three, an oblique ramp superimposed on the border of the sedimentary prism was propagated instantaneously from the backstop to the other side of

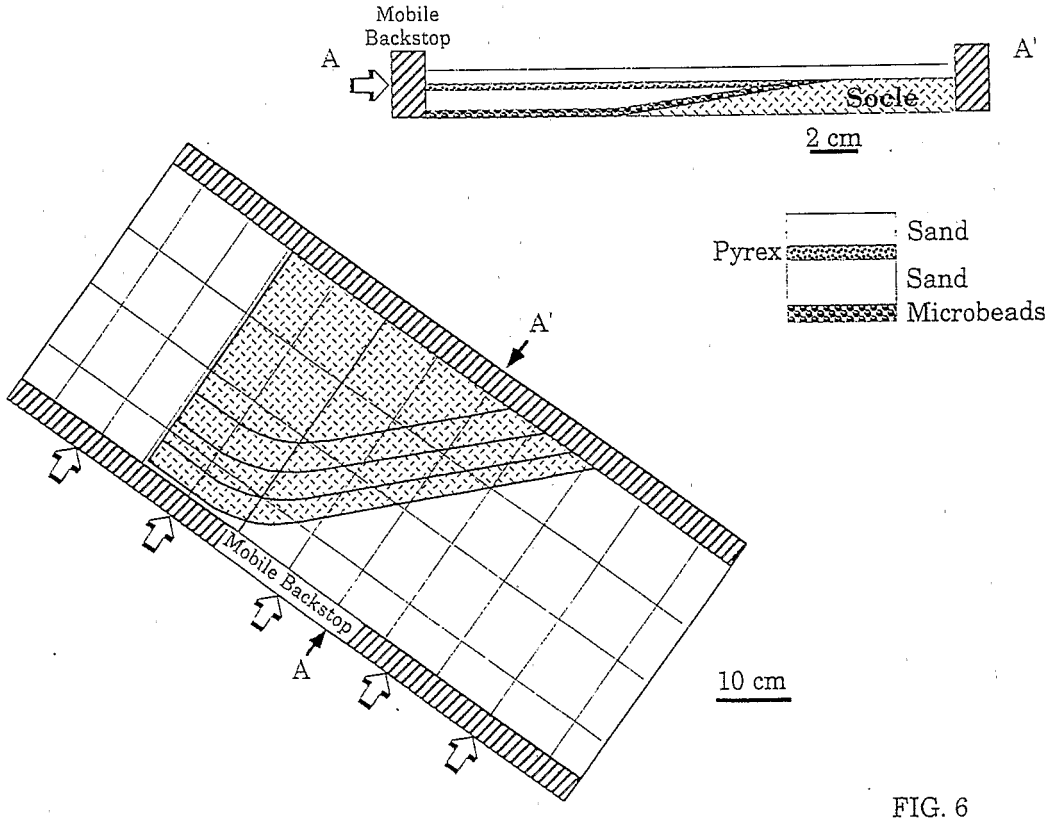

FIG. 6

FIG. 6. Schematic representation of the analog modeling sandbox.

the deformation box. The only way of obtaining a transfer zone similar to the one observed on the structural map of the Boomerang-Chapare area was to use microbeads as the decollement level. This can be accounted for by the mere fact that, in the Boomerang-Chapare area, the decollement occurs in clay levels, whereas silicone putty is used to reproduce ductile deformations and to model rocks such as salt (Cobbold et al., 1989), which does not exist in the Paleozoic in Bolivia. Therefore we will only give the results of the experiment done with the microbeads.

The modeling with microbeads as the decollement level was carlied out with a shortening velocity of 4 cm per hour for 56 minutes, corresponding to a 14% shortening of the model. The deformation stage most faithful to the geometry of the Boomerang-Chapare region was obtained after a 7% shortening of the model (Fig. 7)[1]. It was subjected to a 3D visualization by computerized X-ray tomography.

2.3 Description of the Model at the 7% Shortening Stage

At this stage of the deformation, three imbrications of frontal thrusts linked by two transfer zones with very different geometries can be observed (Fig. 7). These two transfer zones have developed in areas in which the lateral variations in the decollement depth – and therefore of the thickness of the detached series – were rapid.

The first one (Figs 7 and 8a)[1] is located in the central part of the model and has a 40° orientation *vis-à-vis* the compression direction. As in the Boomerang-Chapare area, this oblique ramp ends abruptly in a very short frontal ramp developing toward the thick part of the model. The 3D visualization of the model by computerized X-ray tomography confirms that the oblique ramp is superimposed on the border of the sedimentary wedge (Fig. 9)[1].

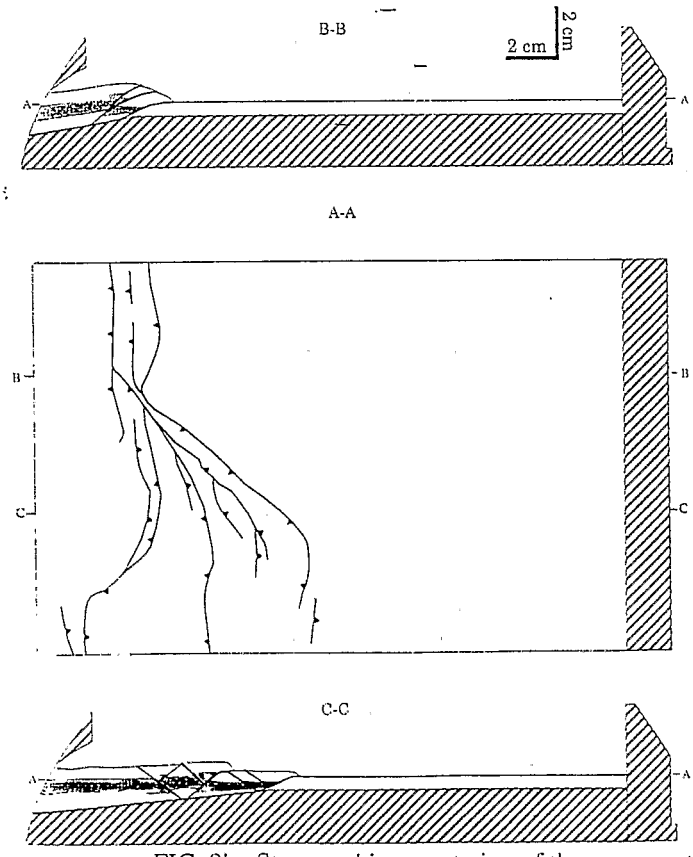

FIG. 9b. Structural interpretation of the cross-sections.

1. See color figures.

The second transfer zone, which is located on the opposite side of the model (Figs 7 and 8b)[1], coincides with the vertical border of the wooden bottom. Its lateral extension is much less than that of the previous one. The geometry of this transfer zone is quite similar to that observed in the field in the Secure region.

These two transfer zones are connected by an imbrication of frontal thrusts (Fig. 7) developing in the zone where the trend of the sedimentary wedge is perpendicular to the shortening direction. This imbrication is characterized by a very great rate of shortening in relation to the thinness of the detached series.

The geometry of the entire deformed model appears very similar to the real geologic structure (Fig. 10).

2.4 Thrust Propagation Time Sequence

To better understand the propagation mechanisms of the Boomerang-Chapare transfer zone, we analyzed the sequence of the development of thrusts by using photographs taken at the various stages of the shortening (Fig. 11)[1]. Up to a shortening of 4.5%, the oblique ramp propagates on roughly half the length of the border of the sedimentary wedge until it ends in a short frontal ramp developing toward the thick part of the model. Simultaneously, a frontal thrust appears in the thick part of the model and propagates laterally towards the oblique ramp. At 4.5% shortening, the tip points of the frontal thrust and of the oblique ramp are on a straight line running parallel to the shortening direction. Between 4.5% and 7% shortening, the oblique ramp

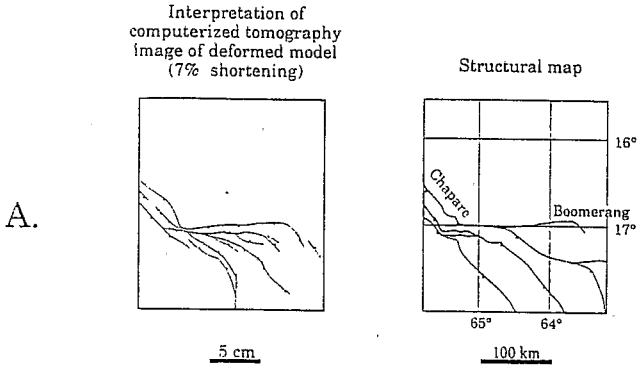

FIG. 10a. Interpretation of the computerized horizontal cross-section of the deformed model after a 7% shortening compared with the structural map of the Boomerang-Chapare area.

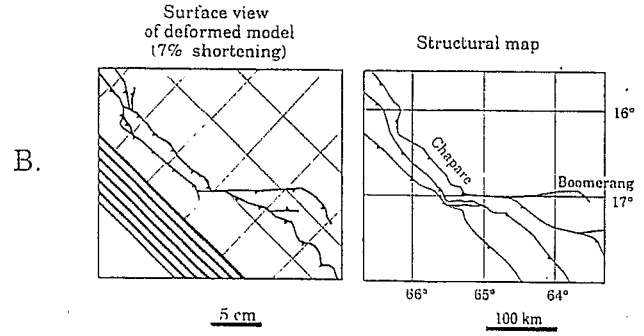

FIG. 10b. Surface view of the model after a 7% shortening compared with the structural map of the Boomerang-Chapare area.

1. See color figures.

ceases to operate, whereas, in back of it, the frontal thrust goes on propagating laterally and connects with the oblique ramp. Thus, if we consider the development in time of the structures on a cross-section that is parallel to the shortening direction and crosses the two ramps, the frontal thrust seems to be out-of-sequence. At 8% shortening, the oblique ramp starts to operate again and keeps propagating along the sedimentary wedge, to end again with a short frontal structure.

3. DISCUSSION

3.1 The Out-of-Sequence Propagation of Frontal Thrusts *Vis-à-Vis* the Oblique Ramp: a Problem of 3D Anisotropic Failure

Deformation analysis has revealed that:

(a) The cylindrical imbrication of thrusts develops in zones where the decollement level depth remains laterally constant.

(b) The front of such imbrications stands all the farther from the mobile backstop since the thickness of the detached series is greater. These results are in full agreement with analog modeling (Mulugetta, 1988) and analytical studies (Davis et al., 1983) showing that, for a given shortening, the front of a collision belt is located all the farther into the foreland as the thickness of the detached series increases.

Yet, the oblique ramp which coinciding to the border of the sand prism (and which simulates the Boomerang thrust front) propagates farther than the frontal ramps developing in the thick part of the model (Fig. 11)[1]. This observation seems to be contradict the rule mentioned above. But it is only an apparent contradiction that can be explained in terms of anisotropic failure (Fig. 12). The bottom of the sand prism, made of glass microbeads,

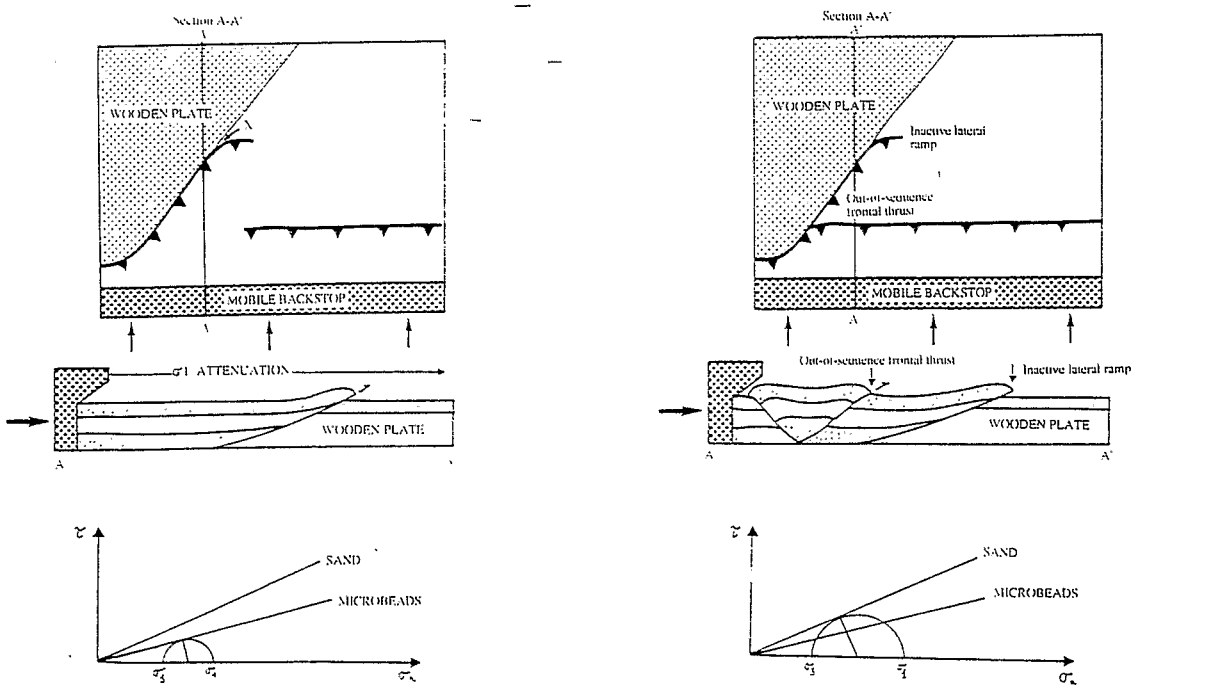

STAGE OF 4.5% SHORTENING: Anisotropic failure at the base of the sand prism. X=limit of the domain of possible anisotropic failure at the base of the sand prism (due to σ1 attenuation).

STAGE OF 7*% SHORTENING: Out-of-sequence isotropic failure in the thick part of the model.

FIG. 12. Mechanical explanation of the out-of-sequence propagation of frontal thrusts *vis-à-vis* the oblique ramp in the Boomerang area.

1. See color figures.

constitutes a surface of anisotropy characterized by an internal friction angle that is smaller (20°) than that of the sand and glass powder layer-cake (33°). Let us consider a cross-section parallel to the shortening direction, crosscutting the sand prism. During compression, the deviatory stress (sigma l-sigma 3) increases, and, as the Mohr circle representation shows, an anisotropic failure will occur along the mechanical discontinuity constituted by the bottom of the prism, until an isotropic failure can develop in the sand and glass powder layer-cake.

On maps (Fig. 11)[1], the oblique ramp then propagates towards the front of the model over a distance depending on the orientation and the dip of the bottom of the prism (it is then a problem of anisotropic failure, which should be treated in three dimensions (Sassi et al., 1993). When the oblique ramp reaches the edge of the domain where the anisotropic failure at the bottom of the prism is made possible, it tries to keep propagating through a frontal structure in the thicker part of the model. However, as the conditions necessary to the isotropic failure are not fulfilled in this part of the model, it fails to propagate, and the oblique ramp ends in a very short frontal structure. With the oblique ramp having stopped operating, the deviatory stress starts increasing again. An isotropic failure will then be able to occur in the thicker part of the model and will lead to the out-of-sequence propagation of frontal thrusts.

3.2 Oil Field Location Depending on Thrust Propagation Sequence

In Bolivia, the central part of the Andean foothills is the zone where, up to now, petroleum exploration has been the most intense. A synthesis of the numerous exploration wells reveals that the structures located along the Boomerang oblique ramp are generally oil bearing, whereas the internal frontal ramp anticlines – like the San Juan structure (Figs 4a and 4b) – are not. This anticline, however favorable (large 3D closure, presence of reservoirs), does not hold any hydrocarbons. These phenomenom can be explained by the thrust propagation sequence.

An analysis of the thrust propagation sequence by analog modeling has shown that, in the Boomerang zone, the internal frontal structures develop in an out-of-sequence way in relation to the oblique ones. The explanation of the distribution of the oil and gas fields would be a migration of hydrocarbons occurring, or at least ending, in the interval of time elapsing between the propagation of the Boomerang oblique ramp and the out-of-sequence formation of the internal frontal structure (Fig. 13). This would explain why the structures of the Boomerang-Chapare trend are oil-bearing whereas the out-of-sequence structure of San Juan is not.

CONCLUSIONS

The transfer zones in the frontal part of the Bolivian Andean thrust belt in the Boomerang-Chapare region were analysed in two complimentary ways: by a regional synthesis and by analog modeling.

Subsurface data have shown that the main decollement level is located at the bottom of the Paleozoic sedimentary series, which lie on the Brazilian shield, and that these series are not isopachous. They have also shown that the Boomerang oblique ramp coincides with the northern border of a Paleozoic sedimentary wedge whose direction runs obliquely to the shortening direction. It was then possible to put forward a hypothesis according to which all the oblique ramps located north of Santa Cruz are associated with lateral variations in the thickness of the detached Paleozoic series and correspond to rapid changes in the decollement level depth. This result is in agreement with the analytical studies of Davis et al., 1983, which show that, for a given amount of shortening, the front of a collision belt is located all the farther into the foreland as the thickness of the detached series increases. The noncylindrical structure of the whole Boomerang-Chapare region then appears to be as a consequence of the lateral thickness variations of the detached Paleozoic basin.

The analog modeling experiments whose 3D visualization was achieved by a scanner enabled us to test and confirm this hypothesis and to study the thrust propagation sequence. The geometry of the deformed

1. See color figures.

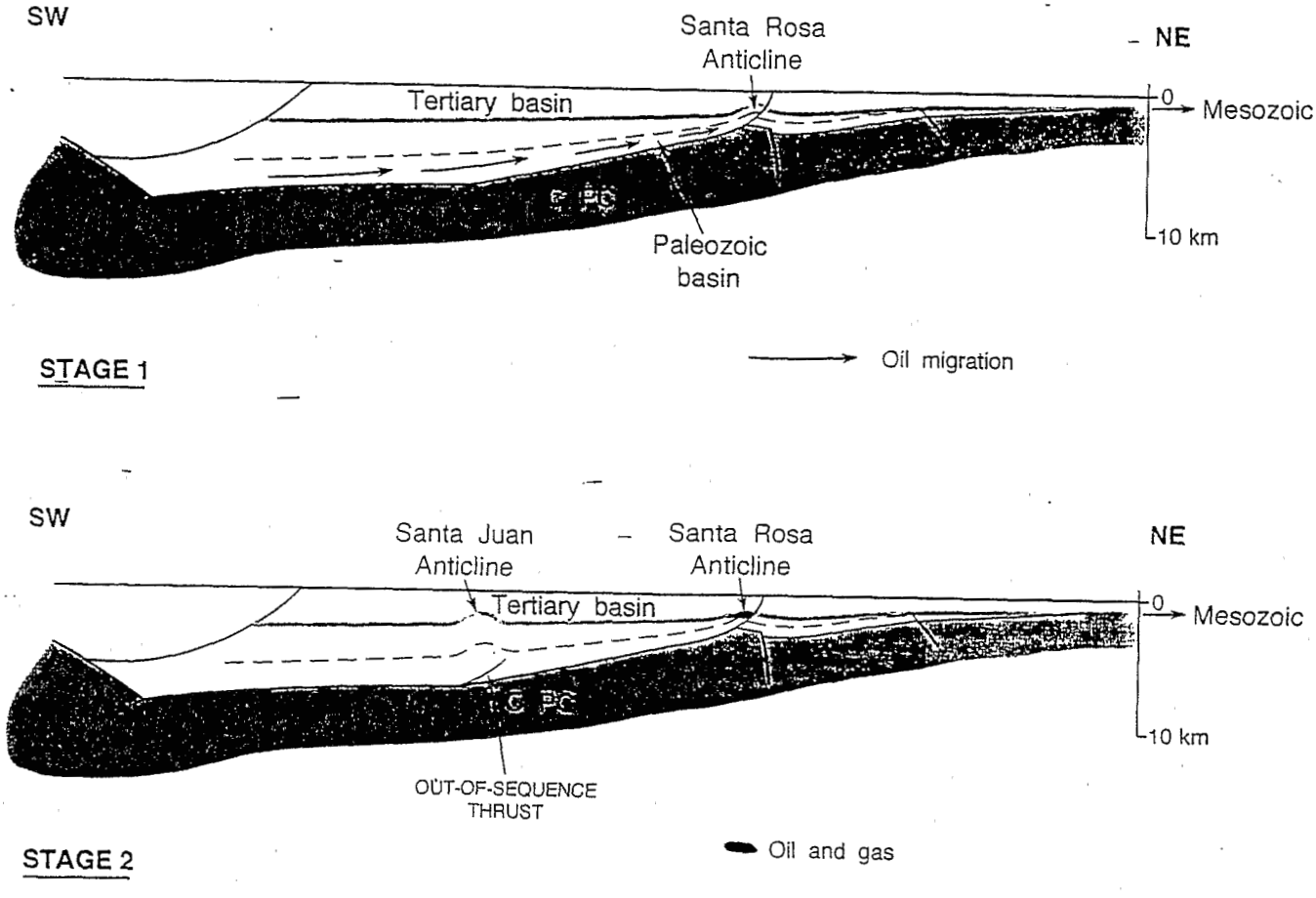

FIG. 13. Explanation of the distribution of oil and gas fields in the Boomerang area in terms of thrust propagation sequence.

model appears very similar to the real geologic structures (Fig. 10). This proves that we have gained a good understanding of the boundary conditions that are the cause of the noncylindlical structures of the Boomerang Chapare region. On cross-sections parallel to the shortening direction, we observed the out-of-sequence development of internal frontal thrusts in respect to oblique ramps. This out-of-sequence propagation can be explained in terms of anisotropic failure along the bottom of the Paleozoic sedimentary wedge.

Concerning petroleum exploration, we have shown how, in the Boomerang-Chapare area, the initial geometry of the Paleozoic wedge controlling an out-of-sequence thrust propagation geometry could be the cause of oil-and-gas field location along the Boomerang oblique ramp.

Finally, on a regional scale, the similarity of the structural map and of the result of analog modeling enable us to propose a geometry of the actual Paleozoic sedimentary basin and of its borders, of which little was known before. The control of the geometry of the Paleozoic sedimentary prism over that of the external part of the Bolivian Andes has been clearly demonstrated, and, as Fig. 14 suggests, the bending of the whole Bolivian Andean thrust belt could be also originated from the geometry and space organization of the entire Paleozoic basins.

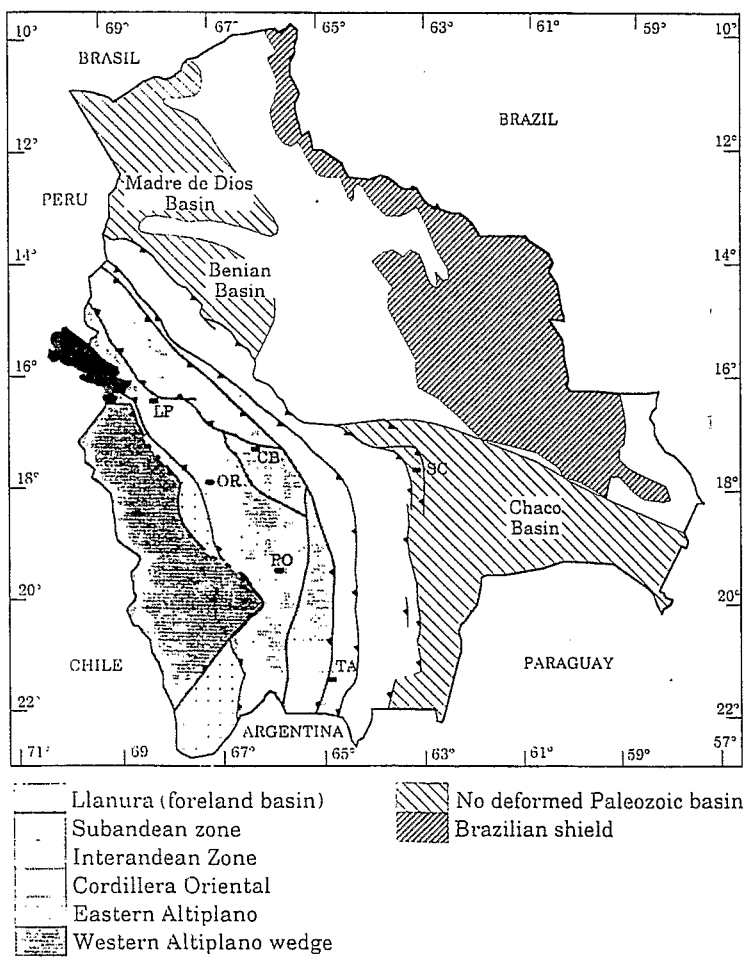

FIG. 14. Is the Bolivian Orocline related to the distribution in space of the Paleozoic basins?

Acknowledgments

We are indebted to YPFB for access and use of seismic profiles and well data.

REFERENCES

Baby P., G. Hérail, J. M. Lopez, O. Lopez, J. Oller, J. Pareja, T. Sempere, D. Tufino, 1989, « Structure de la zone subandine de Bolivie: influence de la géométrie des séries sédimentaires antéorogéniques sur la propagation des chevauchements », *C. R. Acad. Sci.*, **309**, S. II, 1717-1722 (in French).

Baby, P., G. Hérail, R. Salinas, T. Sempere, 1992, "Geometric and kinematic evolution of passive roof duplexes deduced from cross section balancing: example from the foreland thrust system of the southern Bolivian subandean zone", *Tectonics*, **11**, No. 3, 523-536.

Carey, S. W., 1958, "The orocline concept in geotectonics", *Proc. R. Soc. Tasmania*, **89**, 255-258.

Cobbold P., E. Rosselo, B. Vendeville, 1989, "Some experiments on interacting sedimentation and deformation above salt horizons", *Société Géologique de France, Bull.*, **8**, No. 3, 453-460.

Coletta, B., J. Letouzey, R. Pinedo, J. F. Ballard and P. Balé. 1991. Computed X-ray tomography analysis of sandhox models: Examples of thin-skinned thrust systems, Geology, v. 19, 1063-1067.

Dahlstrom, C.D.A., 1969, "Balanced cross sections", *Can. J. Earth Sci.*, **6**, 743-757.

Davis D., Suppe, J., Dahlen, F.A., 1983, "Mechanics of Fold-and-Thrust Belts and accretionary Wedges", *Journ. Geoph. Res.*, **88**, No. B2, 1153-1172.

Isacks, B.L., 1988, "Uplift of the Central Andean Plateau and Bending of the Bolivian Orocline", *Journ. Geoph. Res.*, **93**, No. B4, 3211-3231.

Lopez, J. M., 1974, Correlacion estratigrafica longitudinal de la Faja Subandina entre las fronteras del Peru y Argentina, *Rep. 1906, Yacimientos Fiscales Petroliferos Bolivianos*, Santa Cruz (in Spanish).

Malavielle, J., 1984, « Modélisation expérimentale des chevauchements imbriqués: Application aux chaînes de montagnes », *Société Géologique de France, Bull.*, **7**, 129-138 (in French).

Martinez, C., 1980, « Structure et évolution de la chaîne hercynienne et de la chaîne andine dans le nord de la Cordillère des Andes de la Bolivie », *Trav. Doc. Orstom*, **119**, 352 p., Paris (in French).

Montemurro G., 1992, Desarollo de Facies Sedimentarias del Silurico-Devonico en el Sector Boomerang-Subandino Centro, Bolivia, *Conferencia internacional cuencas Fanerozoicas del Gondwana Sudoccidental*, Santa Cruz (Bolivie), 12-16 agust (in Spanish).

Oller, J., 1986, Concideraciones generales sobre la geologia y estratigrafia de la Faja Subandina norte, *Thèse de l'Université mayor de San Andres*, La Paz, p. 120 (in Spanish).

Padula, E. L., 1959, Valoracion de las discordancias en las Sierras Subandinas, *Bull. Tech. Y.P.F.B.*, **1**, 7-28 (in Spanish).

Pareja, J., Ballon, R., 1978, Mapa geologico de Bolivia, échelle 1/1.000.000, *Yacimientos Fiscales Petroliferos Bolivianos y Geobol*, La Paz (in Spanish).

Sempere, T., Hérail, G., Oller, J., Bonhomme, M.G., 1990, Late Oligocene-early Miocene major tectonic crisis and related basins in Bolivia, *Geology*, **18**, 946-949.

Sassi, W., Colletta, B., Balé, P., Paquerau, T., 1993, Modelling structural complexity in sedimentary basins: the role of preexisting faults *(submitted to Tectonophysics)*.

Sheffels, B., 1988, Structural constraints on crustal shortening in the Bolivian Andes, Ph.D. Thesis, 170 pp., *Mass. Inst. of Tech.*

LEGENDES DES FIGURES COULEURS A COLLER ULTERIEUREMENT

FIG. 7. Photograph and interpretation of the surface of the deformed model (stage of 7% shortening).

FIG. 8. Photograph and interpretation of the transfer zones obtained after a 7% shortening (location in Fig. 7):

(a) On the border of the sedimentary wedge.
(b) On the vertical border of the wooden bottom.

FIG. 9a. Vertical and horizontal cross sections obtained by 3D computerized X-ray tomography after a 7% shortening.

FIG. 11. Photography of the surface view at three different stages of shortening (4.5%, 7% and 8%) showing the thrust propagation sequence. Note that oblique ramps always propagate farther than frontal ones.

7% SHORTENING

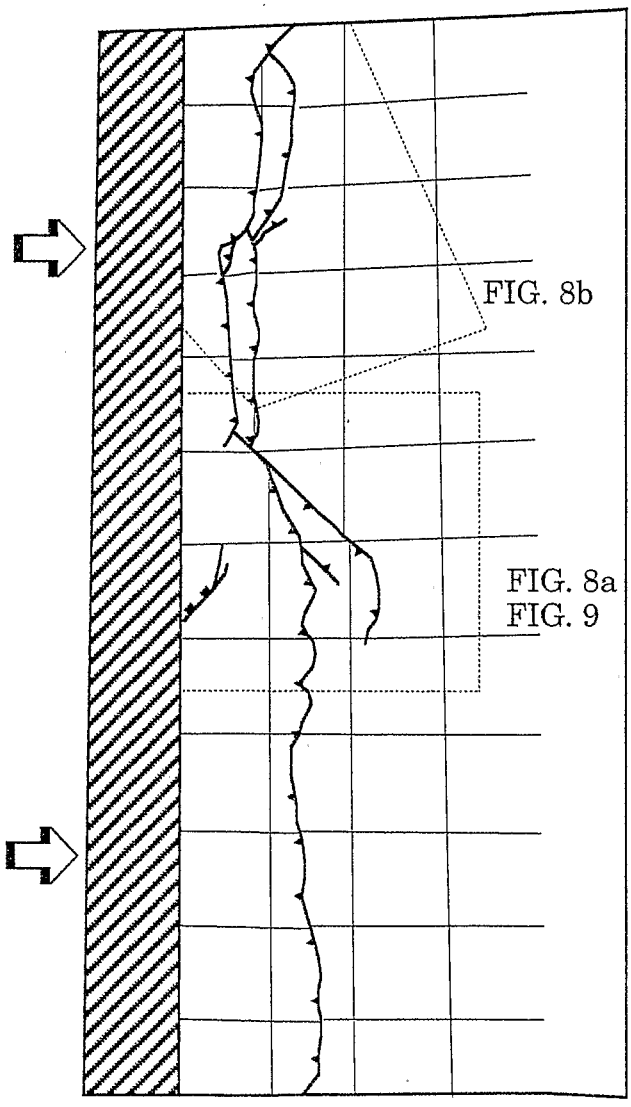

FIG. 7

FIG. 8

7% SHORTENING

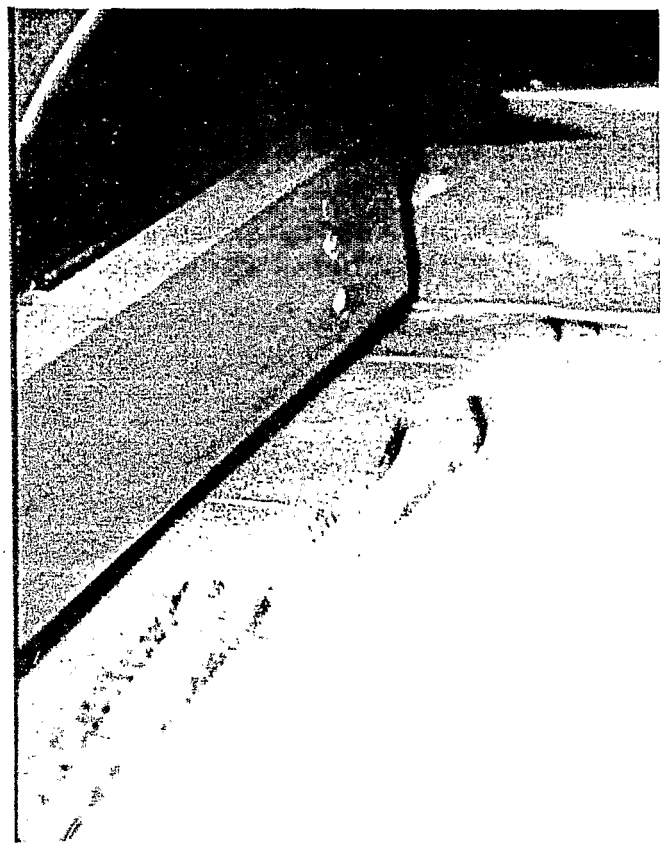

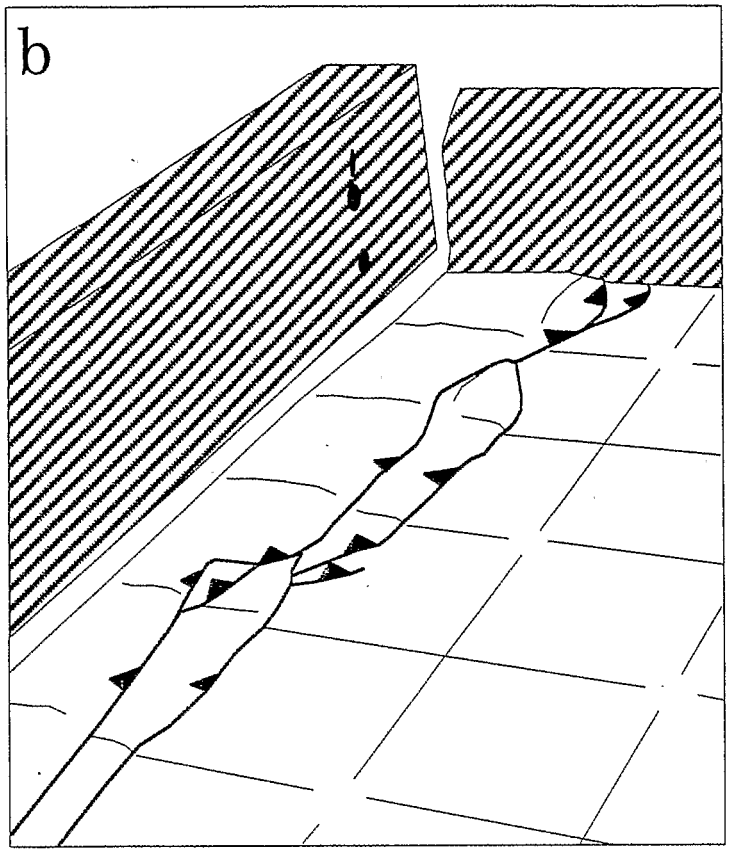

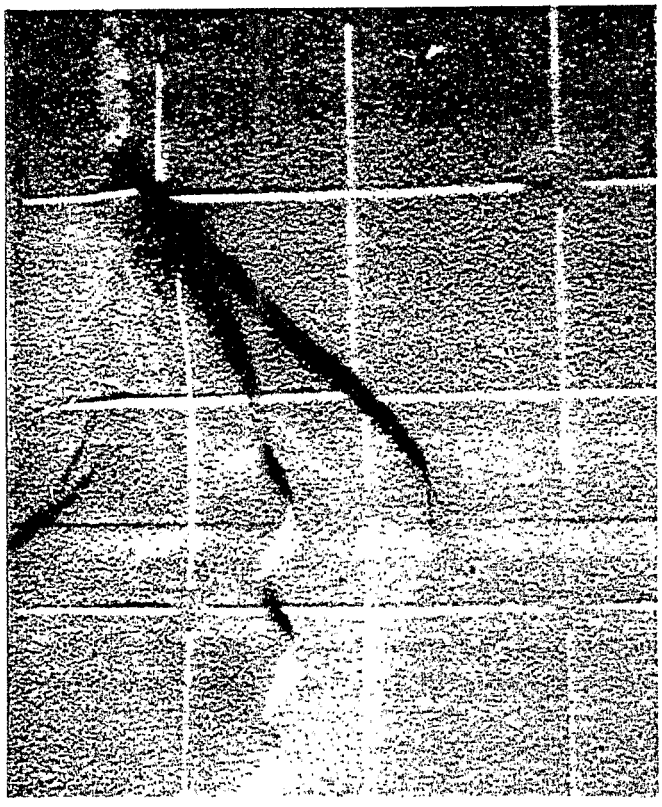

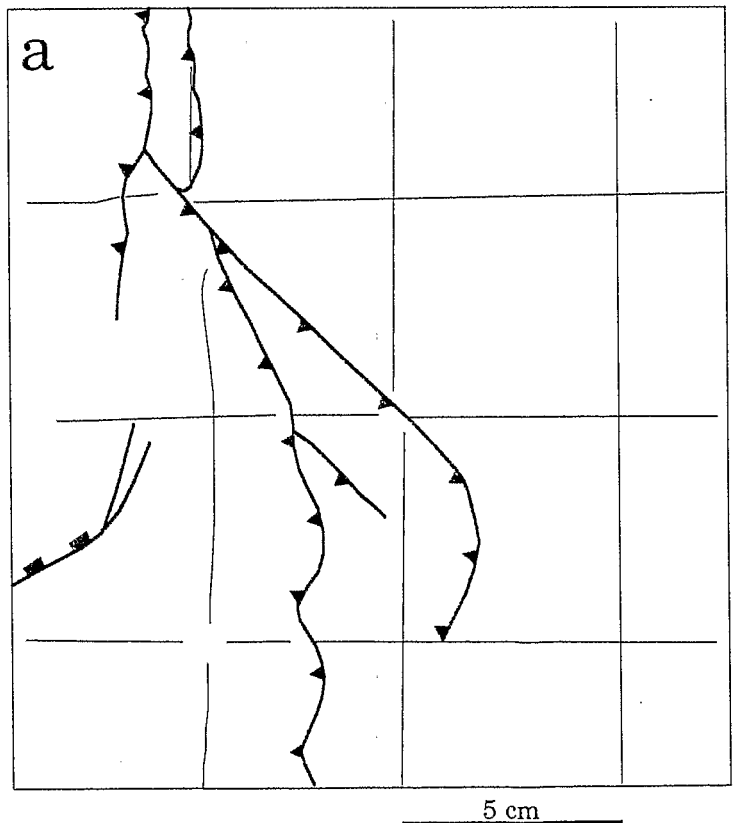

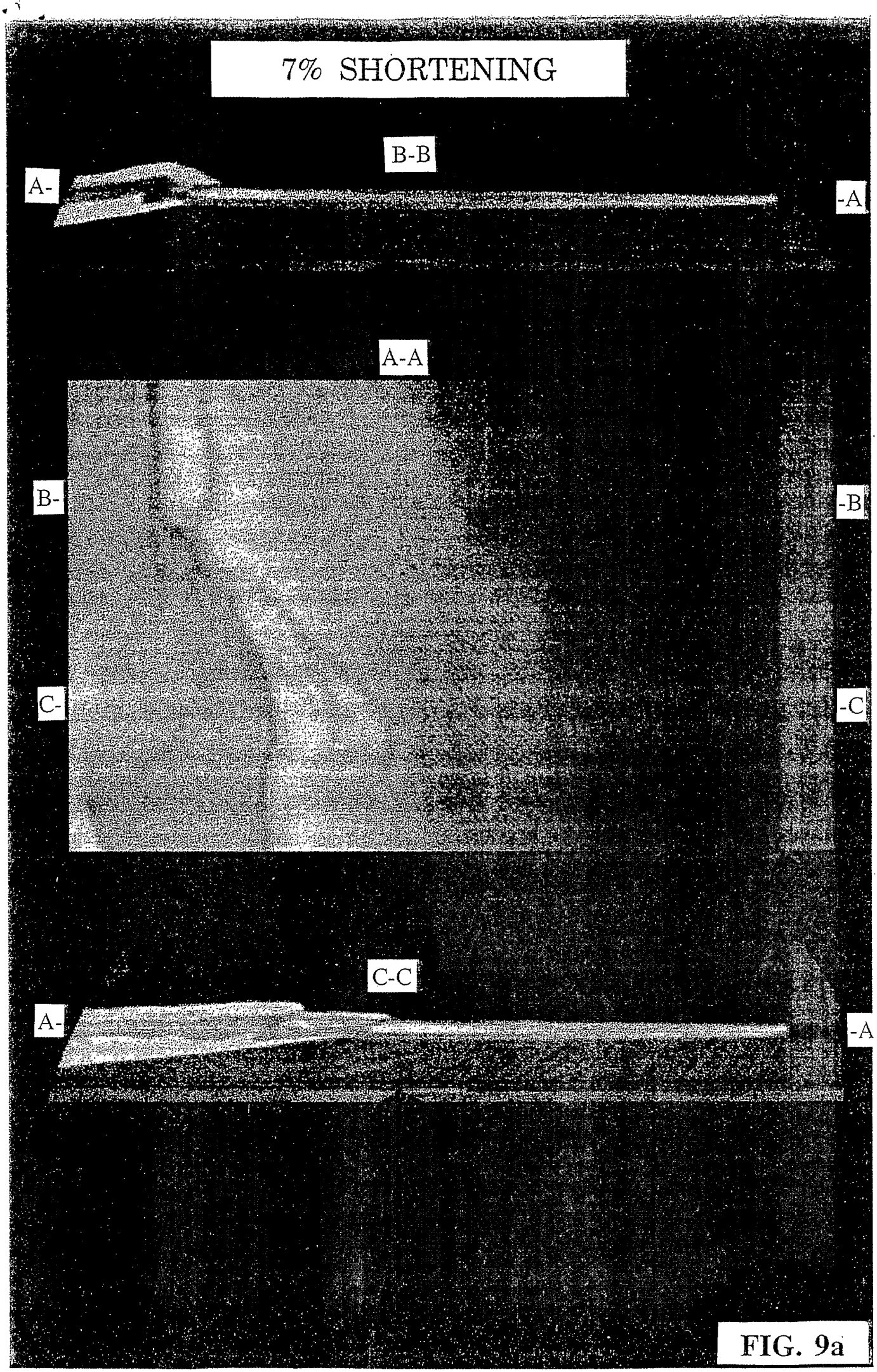

FIG. 9a

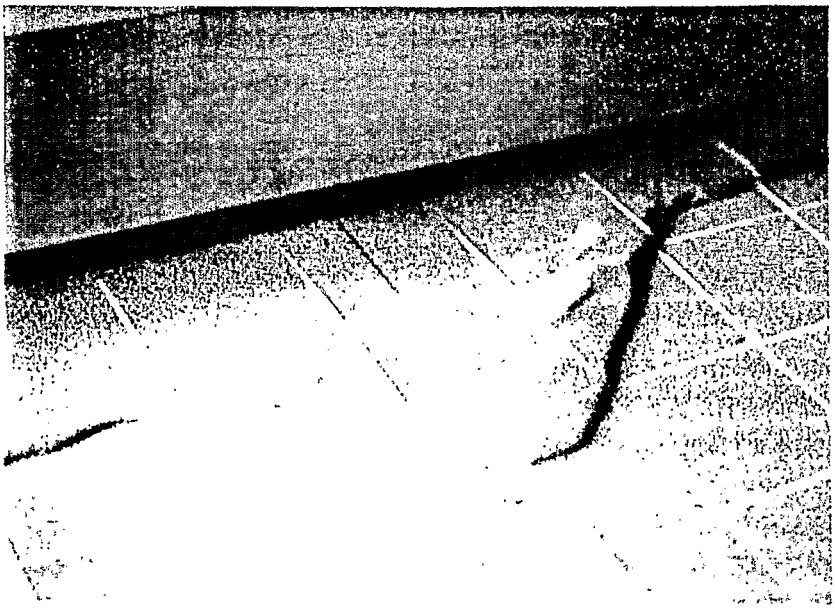

4.5% SHORTENING

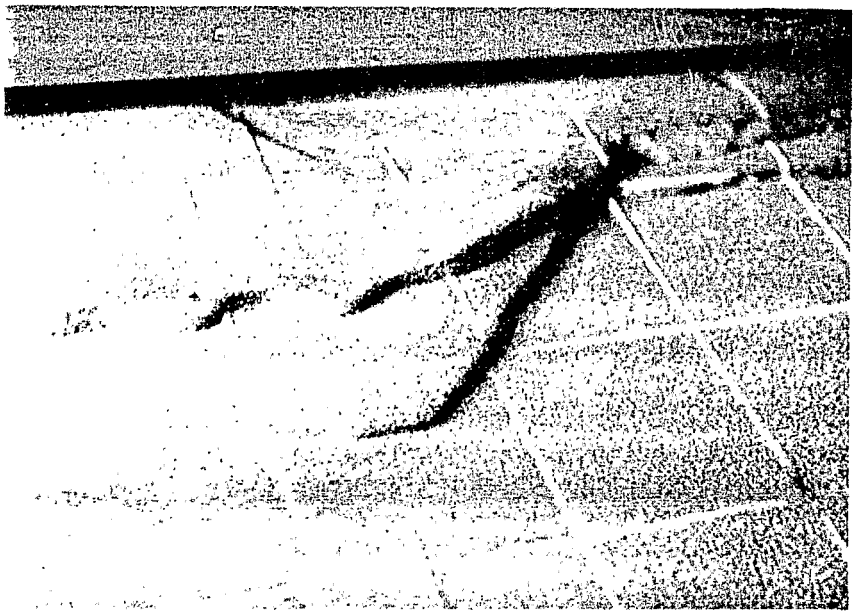

7% SHORTENING

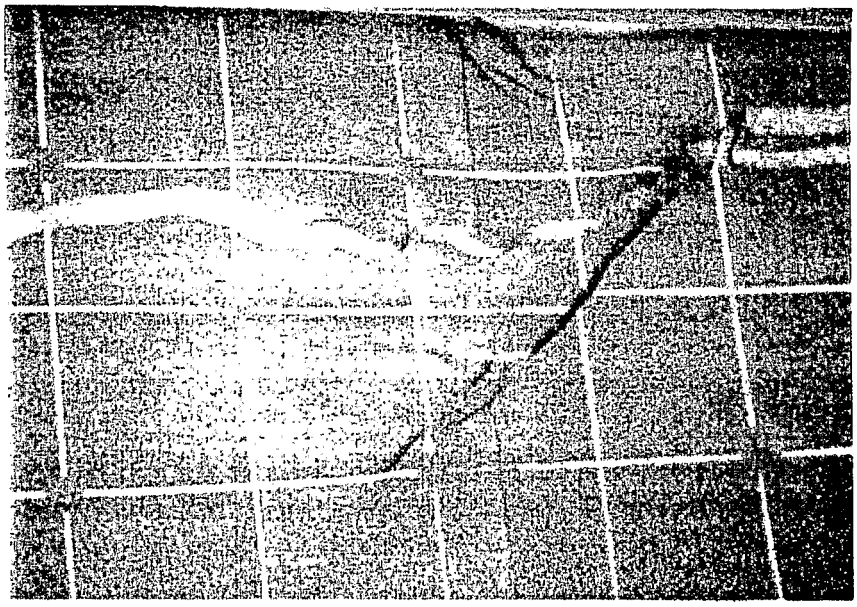

8% SHORTENING

FIG. 11